

RSC Advances



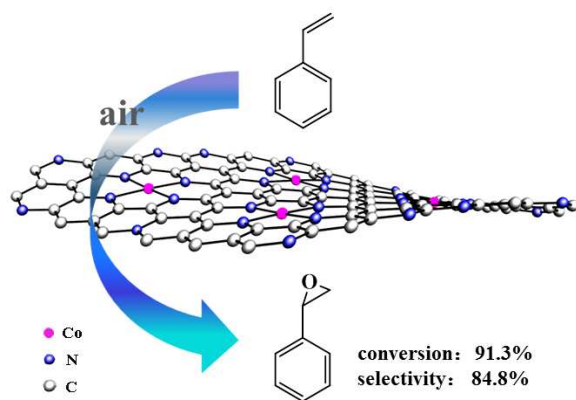
This is an *Accepted Manuscript*, which has been through the Royal Society of Chemistry peer review process and has been accepted for publication.

Accepted Manuscripts are published online shortly after acceptance, before technical editing, formatting and proof reading. Using this free service, authors can make their results available to the community, in citable form, before we publish the edited article. This *Accepted Manuscript* will be replaced by the edited, formatted and paginated article as soon as this is available.

You can find more information about *Accepted Manuscripts* in the [Information for Authors](#).

Please note that technical editing may introduce minor changes to the text and/or graphics, which may alter content. The journal's standard [Terms & Conditions](#) and the [Ethical guidelines](#) still apply. In no event shall the Royal Society of Chemistry be held responsible for any errors or omissions in this *Accepted Manuscript* or any consequences arising from the use of any information it contains.

Table of contents



Novel nitrogen-cobalt catalysts are successfully prepared and exhibit high activity and stability in aerobic epoxidation of styrene without any initiator.

ARTICLE

Cobalt-based metal organic framework as precursor to achieve superior catalytic activity for aerobic epoxidation of styrene

Cite this: DOI: 10.1039/x0xx00000x

Received 00th January 2012,
Accepted 00th January 2012

DOI: 10.1039/x0xx00000x

www.rsc.org/

Guangli Yu,^a Jian Sun,^b Faheem Muhammad,^a Pengyuan Wang^a and Guangshan Zhu^{*a}

Novel nitrogen-cobalt catalysts have been successfully synthesized via one-step pyrolysis of cobalt-based metal organic framework (ZIF-67) at different temperature under inert atmosphere. The influence of the carbonization temperature on the porous structure of the nitrogen-cobalt catalysts is comprehensive investigated through XRD, XPS and N₂ adsorption techniques. Furthermore, the catalytic performance is investigated for epoxidation of styrene using air as the terminal oxidant. The prepared catalysts exhibit excellent styrene conversion (76.2-91.3%) with better epoxide selectivity (81.3-84.8%) in comparison with neat ZIF-67 (39.3%, 79.4%). Advantageously, the magnetically recoverable catalysts could be efficiently reused for 5 times without noticeable deterioration in activity and selectivity. This work provides an elegant approach to the development of cost-effective and practical catalysts for oxidation reactions.

Introduction

Selective oxidation of styrene to corresponding epoxide is a pivotal industrial reaction in the production of both agrochemicals and pharmaceuticals.¹ As we know, it is considerably difficult to activate the carbon-carbon double bonds of styrene because of its high stability. To achieve satisfactory catalytic results, conventional epoxidation process is usually performed with homogeneous transition metal complexes (e.g. binaphthyl complexes, metalloporphyrins complexes, Schiff's base complexes) and hazardous oxidants (e.g. organic peracids, *t*-butyl hydroperoxide).²⁻⁶ The metal complexes based homogeneous catalytic systems inevitably lead to significant metal contamination due to troublesome separation which in turn hampers their commercial value. Alternatively, homogeneous complexes are immobilized onto insoluble solid support to overcome separation problem, but it still requires tedious multistep grafting procedures and harsh synthetic conditions.^{7, 8} In addition, the phenomenon of metal leaching is likely to occur during the catalytic transformation. Consequently, from environmentally friendly as well as economical viewpoint, epoxidation of styrene with eco-friendly oxidants (air/O₂), without using any co-reductant, over efficient catalysts has attracted a tremendous interest in recent years. However, the development of cost-effective, recyclable, and easily separated heterogenized catalyst and its utilization under aerobic conditions are challenging tasks from the perspective of sustainable and green chemistry.

Cobalt-based heterogeneous catalysts are widely applied in epoxidation of alkenes. Particularly, the use of O₂, without any co-reductants, has aroused great interest. Tang et al. first reported that Co (II)-exchanged faujasite-type zeolites could catalyze styrene epoxidation using O₂ as oxidant without any other co-reductants.^{9, 10} Later, Co (II)-exchanged zeolite X, cobalt substituted SSZ-51 and cobalt-substituted SBA-15 were synthesized and applied in alkene epoxidation.¹¹⁻¹³ Nevertheless, the above-mentioned catalytic systems have some drawbacks such as complicated synthetic process, low epoxide selectivity and use of pure oxygen rather than air as terminal oxidant.

Metal-organic frameworks (MOFs) have aroused a considerable attention over the past decade, as they are regarded as a novel generation of ordered porous materials.¹⁴ These intriguing materials are modularly constructed by self-assembly of linking organic ligands with metal nodes or metal clusters to form diverse network structures. Motivated by their permanent porosity, compositional and structural variability, and uniform open cavities, MOFs have been emerged as ideal materials for wide-ranging applications including chemical sensor, gas adsorption, drug delivery, catalysis, and so forth.¹⁵⁻²⁰ They in comparison to purely inorganic porous solids (e.g. zeolites or activated carbon) enjoy many obvious advantages, especially in the field of heterogeneous catalysis. Besides the previously commented designed crystal engineering, the most important one is by introducing a wealthy of catalytically active transition metal-connecting points or additional functional

groups into the porous MOFs structures.^{21, 22} In this regard, MOFs can be directly used in heterogeneous catalysis^{18, 23-25} or post-modified with metal complexes.²⁶⁻²⁸ To date, only a handful of robust Co-based MOFs (STA-12, MFU-1, MFU-2 et al.)²⁹⁻³¹ studies have been reported on epoxidation reactions and achieve satisfactory catalytic results. As we all know, the relatively low chemical and thermal stability of porous MOFs prevented their development. Taken together, the synthesis of robust metal-organic frameworks as heterogeneous catalysts with potential application is still a challenging research goal.

In order to fabricate the required material, we reported a new experimental strategy, using porous MOF as sacrificial template, to prepare catalyst for styrene oxidation. In this approach, the inexpensive cobalt imidazolate frameworks (ZIF-67) are selected as the premier candidate, which had been used for capacitor and water treatment.^{32, 33} Structurally, as depicted in Figure 1, each cobalt center is coordinated to four nitrogen atoms of imidazolate ligands, thus forming regularly distributed Co-N₄ moieties within the frameworks. After carbonization under inert atmosphere, catalysts are acquired with Co-N₄ macrocycles on a carbon support, while still maintain the porous framework. The catalysts possess uniformly distributed active sites with high surface area. Furthermore, the presence of metallic Co⁰ provided an added opportunity to magnetically separate catalysts from the reaction mixture. As elaborated in previous work,³⁴ O₂ molecules can be adsorbed on the central transition metal atom (Co) of the Co-N₄ clusters. More importantly, transition metal with variable chemical valence, can transfer electronic effect which is confirmed to be the main active site as oxygen transfer agents. When applied as catalytic material, the porous Co-N₄ complexes provided heterogeneous catalytic sites for the selective oxidation of styrene to epoxide even using benign air as the final oxidant. Unexpectedly high conversion (91.3%) and good epoxide selectivity (84.8%) have been obtained using ZC-700 as catalyst at an optimized temperature. Gratifyingly, catalysts are magnetically separated and reused 5 cycles with insignificant loss in catalytic activity and selectivity.

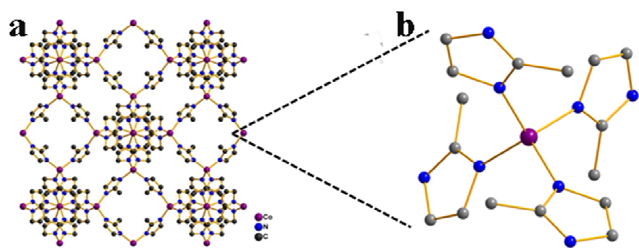


Fig. 1. (a) structural packing of ZIF-67 along the a axis direction; (b) enlarged Co-N₄ coordinated moiety.

Experimental

Materials and methods

Cobalt nitrate hexahydrate (Co (NO₃)₂·6H₂O, Sinopharm Chemical Reagent Co., Ltd., China, AR), 2-methylimidazole (MeIM, Chengdu Kelon Chemical Reagent Factory, AR),

triethylamine (C₆H₁₅N, Tianjin Fuyu Chemical Co., Ltd., AR), styrene (Sigma-Aldrich, 98%) N, N'- dimethylformamide (DMF, Beijing Chemical Works, AR) and distilled water are used as received without any further purification.

The powder X-ray diffraction (XRD) measurements were performed on a Rigaku D/MAX 2550 diffractometer using Cu-Kα radiation (λ = 1.5418 Å) and operating at 50 KV and 200 mA, with a scanning step of 0.02°. X-ray photoelectron spectroscopy (XPS) was carried out on Scienta ESCA200 spectrometer using Al-K α radiation. For porosity analysis, nitrogen adsorption-desorption experiments were taken at 77 K on an Autosorb iQ2 adsorptometer, Quantachrome Instrument. Prior to the tests, the samples were degassed overnight at 423 K under high vacuum. Specific surface areas were calculated by using the Brunauer-Emmett-Teller (BET) equation; and the pore size distributions were determined by applying non-local density functional theory (NL-DFT) methods respectively. The metal content of all the catalysts was analyzed by inductively coupled plasma atomic emission analyses (ICP-AES, Perkin-Elmer Optima 3300 DV). The magnetic properties were measured by a superconducting quantum interface device magnetometer (SQUID VSM) at room temperature.

Synthesis of ZIF-67 nanocrystals

ZIF-67 (Co-MOF) nanocrystals in this work were prepared following a previously reported method with a slight modification.³⁵ Briefly, Co(NO₃)₂·6H₂O (0.717 g, 2.46 mmol) was dissolved in H₂O (50 mL), and meanwhile, 2-methylimidazole (3.244 g, 39.5 mmol) and triethylamine (4 mL) were dispersed in another H₂O (50 mL). Afterwards, both solutions were rapidly mixed together, and continued stirring for overnight with a magnetic bar at room temperature. Finally, the purple powders were purified by repetitive centrifugations (10000 rpm, 2 minutes) using H₂O as the solvent with subsequent drying in air.

Preparation of heterogeneous catalysts

As-made ZIF-67 samples were placed inside a quartz boat, which was introduced in the middle of a quartz tube with both ends connected to argon gas. The tubular furnace was heated up at different temperatures ranging from 600 to 900 °C for 5 hours under continuous argon flow of 50 mL min⁻¹ with a heating ramp of 1° min⁻¹. After natural cooling to room temperature, the resultant catalysts were obtained and designed as ZC-T, where T referred to carbonization temperature (600, 700, 800 and 900 °C).

Catalytic epoxidation of styrene

Styrene epoxidation with air was performed in a two necked flask (50 mL) equipped with a liquid condenser and air pump. In a typical procedure, styrene (2 mmol) as substrate and the nanocatalysts (50 mg) were added into DMF solution (8 mL). Then the mixture was refluxed at optimized temperature for 6 h, and air was introduced with a stable flowing rate of 80 mL min⁻¹. After completion of the reaction, the nanocatalysts were recovered by a magnet, washed with acetonitrile and ethanol,

dried at vacuum and reused without further purification. The products of epoxidation reaction were quantified and monitored *via* gas chromatography (Shimadzu, GC-8A) equipped with a HP-5 capillary column and a FID detector. The reaction kinetics was monitored via withdrawing 0.1 ul of the reaction liquid at 0.5h intervals and analysing the measurements by GC. Calibration of GC peak areas of styrene and epoxide was done through solutions with known amounts of styrene and epoxide in DMF. The conversion was calculated on the basis of molar percent of styrene; the initial molar percent of styrene was divided by initial area percent to get the response factor. The unreacted moles of styrene remaining in the reaction mixture were calculated by multiplying the response factor by the area percentage of the GC peak for styrene obtained after the reaction.¹¹ In the most reaction conditions, styrene polymerization was negligible, thus polymers in the reaction products were not considered.³⁶ The conversion of styrene, selectivity, yield of the products were calculated using the formulae:

$$\text{Styrene conversion (\%)} = ((\text{initial mol\%}) - (\text{final mol\%})) / (\text{initial mol\%}) \times 100$$

$$\text{The product selectivity (\%)} = \text{GC peak area of the product} / \text{GC peak area of all products} \times 100$$

$$\text{The product yield (\%)} = \text{Styrene conversion (\%)} \times \text{the product selectivity (\%)}$$

Results and discussion

XRD measurements

The crystalline structures of as-prepared ZIF-67 and their corresponding C-N-Co nanocomposite materials (labeled as ZC-600, ZC-700, ZC-800, and ZC-900) with varying carbonization temperature are analyzed by powder X-ray diffraction (XRD), where the number (600, 700, 800 or 900) refers to the carbonization temperature. As shown in Fig. 2a, the XRD diffractogram of as-prepared Co-MOF displays high phase purity, which agrees with the well-known simulated ZIF-67 crystal structure. As can be seen from Fig. 2b, shows that all the samples after annealing undergo structural transformation and no longer preserve long-range ordered structure. Meantime, they exhibit similar patterns except increasing intensity of XRD peaks. It can be clearly seen that characteristic carbon (002) broadened peaks around at 25° (2θ) signifies the carbonaceous material formation upon thermal activation of the ZIF-67 precursor. The other peaks at 44.2°, 51.5° and 75.9° can be well ascribed to (111), (200) and (220) lattice facets of the β-Co, respectively, associated with standard JCPDS card no. 43-1003. Additionally, the carbonization temperature has a strong effect on the degree of the metallic Co. We can state that, with increasing annealing temperature, the diffraction peaks become stronger and sharper. These results presumably imply that most of the Co²⁺ ions break away from the ZIF-67 frameworks and then resulting nanoparticles undergo further coalescence to form larger metallic Co particles.³⁷

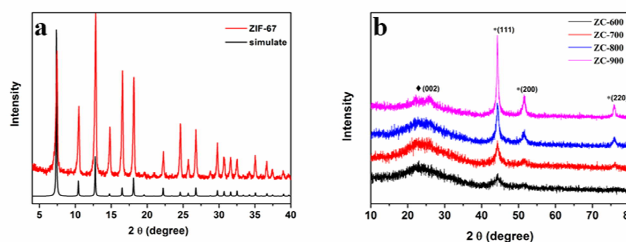


Fig. 2. XRD patterns of (a) as-prepared ZIF-67 and (b) the corresponding C-N-Co hybrid materials at different carbonization temperatures: carbon (♦) and metallic Co (*).

Adsorption measurements

The textural properties of parent ZIF-67 and C-N-Co catalysts are determined by N₂ adsorption-desorption isotherms at 77 K (Fig. 3) and the related parameters are listed in Table S1. Obviously, the curve of ZIF-67 is typical type-I isotherm, indicating that the ZIF-67 precursor is mainly microporous characteristics. After the carbonization reaction, ZC-600, ZC-700, ZC-800 and ZC-900 exhibit N₂ isotherms close to type-IV with small hysteresis loops, which suggest the presence of mesopores in the obtained carbon framework. The value of S_{BET} decreases from 282 to 94 m²g⁻¹ with thermal treatment temperature increasing from 600 °C to 900 °C (Table S1), originating from the emission of carbon from specific edge areas at elevated temperature. As previously reported,³⁷⁻³⁹ metallic cobalt still remains in the carbon skeleton, which indirectly reduces BET values. The pore size distribution (PSD) curves give a plenty of information regarding the assignment of different pore sizes (Fig. 3b). As expected, the pore size of freshly prepared ZIF-67 precursor is distributed merely in micropore region (8 to 11 Å), of which one outstanding point is the emergence of bimodal pore distribution after heat-activated samples at different temperature. Similar to ZIF-67 precursor, a noteworthy fraction of micropores (10 - 16 Å) in C-N-Co catalysts is formed, and mesopores mainly ranging from 20 to 40 Å are also observed. This bimodal distribution may arise from the breakdown of ZIF-67 precursor to form carbonaceous structure.

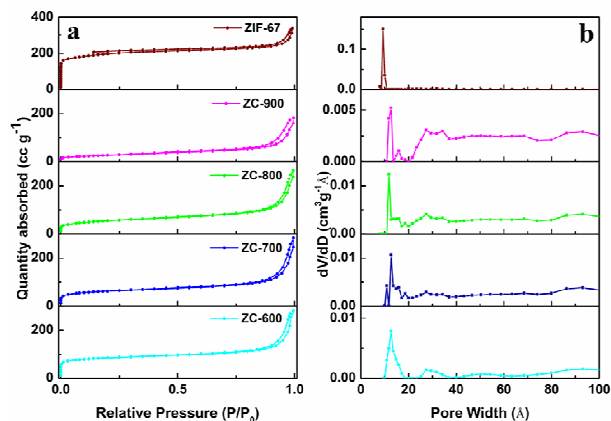


Fig.3 (a) Nitrogen adsorption-desorption isotherms and (b) corresponding NL-DFT pore size distributions of ZIF-67, ZC-600, ZC-700, ZC-800 and ZC-900 catalysts.

Magnetism measurements

The magnetic properties of the nanocomposite materials (C-N-Co) are studied at room temperature with a vibrating sample magnetometer (VSM) (Fig. 4). The synthesized C-N-Co nanoparticles display a representative hysteresis loop, indicating the ferromagnetism feature of them (Fig. 4a). The magnetization saturation (M_s) values of ZC-600, ZC-700, ZC-800 and ZC-900 are found to be 49.6, 59.1, 74.1 and 93.4 emu g^{-1} , respectively. These differences are possibly caused by the crystallinity of the magnetic Co^0 particles under different carbonization temperatures, which also has been corroborated by XRD analysis. More importantly, the dispersed aqueous solution of ZC-700 material can be quickly attracted towards a regular magnet ($< 15\text{s}$), leaving the solution transparent and clear (inset of Fig. 4b). Following the removal of outside magnetic field, the ZC-700 material can be quickly redispersed by slight shaking, illustrating a strong magnetic susceptibility for efficient redispersibility and magnetic responsiveness.

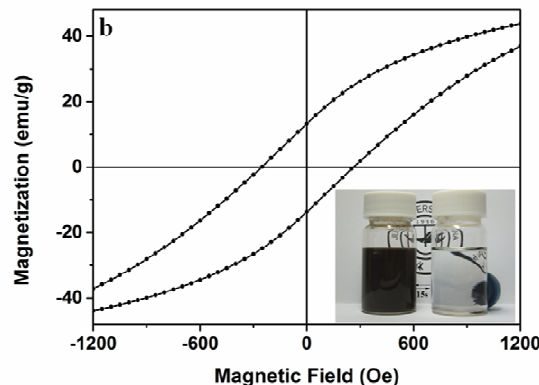
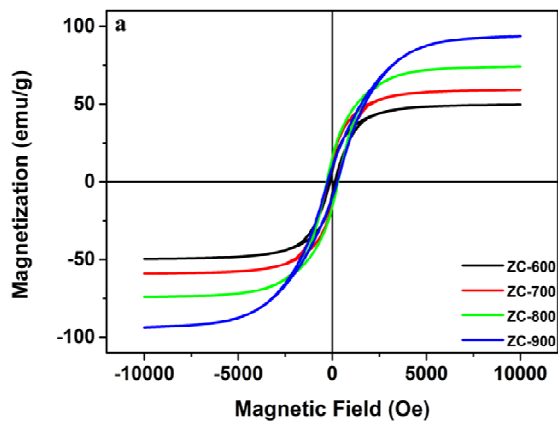


Fig.4. (a) M–H curves of the C-N-Co composites formed by annealing at different temperatures (600 °C, 700 °C, 800 °C, and 900 °C) and (b) an enlarged curve for ZC-700 catalyst.

XPS measurements

To better understand the active sites of catalyst, it is of great importance to investigate the nitrogenous species on the carbon surface before and after heat-treatment ZIF-67 precursor *via* X-ray photoelectron spectroscopy (XPS) (Fig. 5). The images of the full spectrum of the samples are collected in Fig. 5a. The percentage of nitrogen for ZIF-67, ZC-600, ZC-700, ZC-800, and ZC-900 is calculated from survey spectra to be around 15.07, 8.22, 5.09, 2.53 and 1.65%, respectively. It is reasonably surmised that more N atoms will overflow with the increase of pyrolysis temperature. In Fig. 5b-f, the N1s region spectra are deconvoluted into three components: N1 (pyridinic-N), N2 (Co-N_x) and N3 (graphitic-N) that are shown schematically in Fig. S1 and the distributions of the three species of nitrogen atoms are particularly compiled in Table 1. Remarkably, the intensity of these three peaks significantly depends on the annealing temperature evolution. From Fig. 5b, for starting material ZIF-67, the existence of only peak at N2 (BE 399.1 eV) corresponds to N of 2-methylimidazole ligand thoroughly coordinated to Co. After annealing, the other two peaks of N1 (BE 398.5 eV) and N3 (BE 401.1 eV) appear, whereas N2 peak becomes weaker due to 2-methylimidazole ligands ring opening in Fig. 5c-f. Upon further increasing the pyrolysis temperature for ZC-800 and 900 (Fig. 5e and f), the percentage composition of the N2 and N1 peak becomes much lower, whereas the peaks of N3 rise dramatically. This confirms that the formed N3 is much more stable than N1 at high temperatures in accordance with the previous reported.⁴⁰ Among them, ZC-700 presents the highest assignment of N1, accompanied with a high quantity of N2 (Table 1). Based on this analysis, appropriately arranged N1 (pyridinic N) moieties with electron-donating properties are able to trap plentiful transitional metals to serve as outstanding metal-coordination (Co-N_x) active sites.⁴¹ Furthermore, free N1 atoms have excellent electronic storage ability to activate molecular oxygen under mild conditions. ZC-700, herein,

probably have a better catalytic activity, and thus it will be further discussed later.

promising applications in the selective epoxidation of styrene (see below).

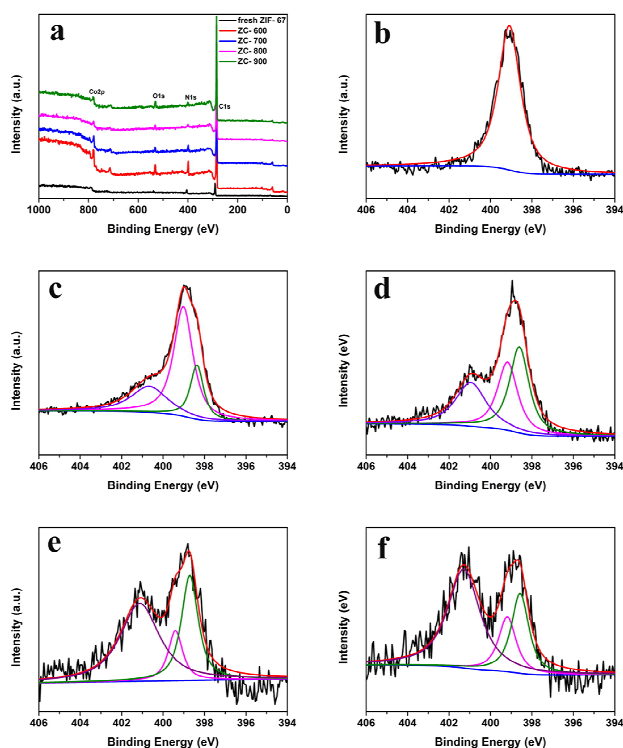


Fig. 5 (a) XPS survey spectra of fresh ZIF-67 and C-N-Co composites. (b-f) High-resolution XPS spectra of the deconvoluted N1s peak: (b) ZIF-67, (c) ZC-600, (d) ZC-700, (e) ZC-800, and (f) ZC-900.

Table 1 Ratio analysis of C, O, Co and heterocyclic N components of all as-prepared samples from XPS analysis.

Sample	C (%)	O (%)	Co (%)	N (%)			
				Total	N1	N2	N3
ZC-600	86.3	3.48	1.93	8.22	19	56	25
ZC-700	90.5	2.5	1.8	5.09	38	31	30
ZC-800	94.15	2.12	1.21	2.53	32	13	55
ZC-900	91.46	5.31	1.58	1.65	25	17	58
ZIF-67	74.92	5.29	4.72	15.07	-	100	-

The Co2p XPS spectra of all samples are also shown in Fig. 6. As depicted in Fig. 6a, metallic Co⁰ (BE 778 eV) can be detected from ZC-600, ZC-700, ZC-800 and ZC-900, respectively, compared to ZIF-67 precursor, which is in accordance with XRD and magnetism results. After deconvolution for the Co2p (Fig. 6b), the dominant peak of ZC-700 catalyst is seen at ~ 781.2 eV, where is on the account of forming the N-coordinated metal (Co-N_x)^{42, 43} which serves as an effective activity center. Undoubtedly, the formation of Co-N bonds in nitrogen-cobalt macrocyclic catalyst shows

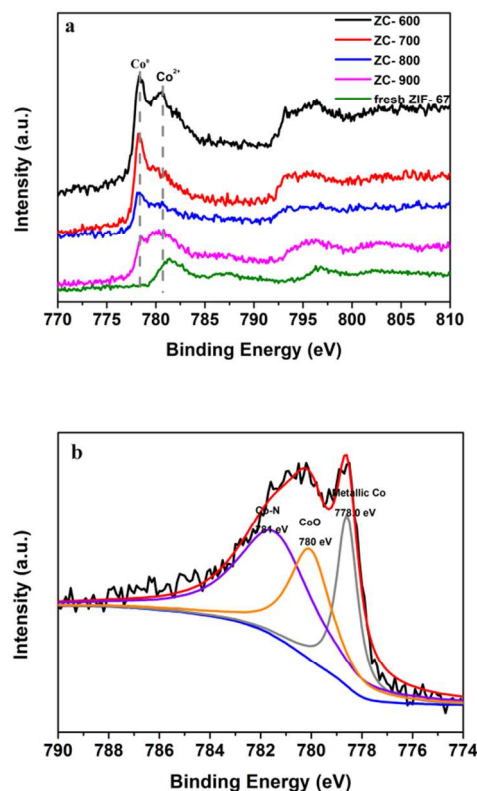


Fig. 6 (a) XPS Co2p spectra of the studied samples and (b) XPS Co2p spectra of ZC-700 catalyst.

Catalytic properties

As-synthesized catalysts with varying carbonization temperature have been utilized for the selective epoxidation of styrene using low-cost air as only oxidant to evaluate the catalytic performance and to understand the temperature selective catalytic activity. Table 2 lists the epoxidation of styrene over various cobalt-based catalysts. For the pure ZIF-67, 79.4% of epoxide selectivity is acquired when air is used, but the styrene conversion (39.3%) is extremely low presumably due to the poor electron storage or transfer nature of the organic framework. To our delight, the catalytic activity is obviously improved when ZIF-67 precursor is heat-activated under argon atmosphere at different temperatures, as is shown in Table 2. In detail, the conversion efficiency of styrene is enhanced from low (76.2% for ZC-600, entry 2) to maximum (91.3% for ZC-700, entry 3) before returning to low (77.1% for ZC-900, entry 5) again. These promising results strongly demonstrate the dependence of catalytic reaction on annealing temperature; moreover, different catalytic sites also affect the epoxidation of styrene activity. It is intriguing to note that ZC-700 catalyst exhibits especially high activity in terms of both high conversion (91.3%) and good epoxide selectivity (84.8%). The excellent catalytic results of ZC-700 sample maybe ascribed to

Table 2 Various catalysts in epoxidation of styrene with air.^a

Entry	Catalyst	Con. (%)	Product selectivity (%)		Product yield (%)	
			Epoxide	Benzaldehyde	Epoxide	Benzaldehyde
1	ZIF-67	39.3	79.4	20.6	31.2	8.1
2	ZC-600	76.2	81.3	18.7	61.9	14.3
3	ZC-700	91.3	84.8	15.2	77.4	13.9
4	ZC-800	84.2	83.5	16.5	70.3	13.9
5	ZC-900	77.1	82.6	17.4	63.7	13.4
6 ^b	ZC-700	27.1	76.3	23.7	20.7	6.4
7 ^c	ZC-700	41.9	75.4	24.6	31.6	10.3
8 ^d	ZC-700	92.5	79.8	20.2	73.8	18.7

^a Reaction conditions: styrene (2 mmol), DMF (8ml), catalyst (50mg), flow rate of air (80ml/min), reaction time (5h), reaction temperature (100 °C). ^b The reaction was performed at 80 °C. ^c The reaction was performed at 90 °C. ^d The reaction was performed at 110 °C.

Table 3 Comparison of ZC-700 with earlier reported Co-containing heterogeneous catalysts for aerobic epoxidation of styrene

Entry	Catalyst	Oxidant	Con. (%)	Epoxide selectivity (%)	References
1	ZC-700	air	91.3	84.8	This work
2	Fe ₃ O ₄ @SiO ₂ -Co	air+ isobutyraldehyde	90.8	63.7	47
3	Co ₃ O ₄	air + TBHP	81.8	84.1	48
4	Co-5A	air + TBHP	89.4	90.2	49
5	Co-SSZ-S-10	O ₂	24	62	13
6	Co ²⁺ -X	O ₂	44.2	60	10
7	Co ²⁺ -NaX	O ₂	44	60	9
8	Co ²⁺ -MCM-41	O ₂	45	62	9

the following reasons. The higher content of N1 and N2 in ZC-700 catalyst (Table 1) than other C–N–Co catalysts might be responsible for the higher catalytic performance, since catalytic active center (Co–N₄ structure) of it promotes the activation of O₂ molecules. Nevertheless, ZC-800 and ZC-900, with low content of nitrogen, therefore demonstrate less activity. Furthermore, some reports^{44, 45} have elaborated this activity by stating that the nitrogen atoms containing units could pointedly enhance the electron-donor capability *via* conjugated π -system of carbon matrix, resulting in promoting the interaction between catalysts and reactants. Lastly, the Co–N_x moieties are stabilized only under lower temperature.^{41, 46} Such issues indicate that ZC-700 catalyst possesses the highest catalytic property and further studies are thus performed with ZC-700 as oxidation catalyst. In addition, DMF plays an important role in aerobic epoxidation styrene, and coordination of DMF with cobalt (II) sites can promote the activation of O₂ molecules to form an active intermediate, which further interact with styrene to produce epoxide.

The temperature dependence study of the epoxidation reaction is also carried out (Table 2, entries 6–8). It is obvious that the styrene conversion and epoxide selectivity sharply increase with an increase of the reaction temperature from 80 to

100 °C, while the epoxide selectivity starts to somewhat decrease at higher temperature (110 °C). This result demonstrates that reaction temperature has great influence on catalytic performance. High temperature is contributed to reaction proceed, but further elevating temperature readily triggers deep oxidation, and accordingly leads to lower epoxide selectivity. In the course of this study, 100 °C is found an appropriate reaction temperature for maximum activity.

The catalytic performance of ZC-700 catalyst for aerobic epoxidation of styrene is compared with earlier reported Co-containing heterogeneous catalysts (Table 3). It is obvious that ZC-700 catalyst gives the highest styrene conversion (91.3%) and good epoxide selectivity (84.8%) without any initiator. From entry 5 to 8, Co-containing heterogeneous catalysts show relatively poor styrene conversion and low epoxide selectivity. From entry 2 to 4, though Co-containing heterogeneous catalysts achieve satisfactory styrene conversion and epoxide selectivity, they have to use hazardous and expensive initiator (TBHP or isobutyraldehyde) as sacrifice, which is far away from the viewpoint of economic and green chemistry. These results corroborate that ZC-700 catalyst acts as an efficient catalyst in aerobic epoxidation of styrene with air as oxidant.

In order to further elucidate the catalytic activity, recycling tests of ZC-700 catalyst are conducted and the obtained results are shown in Fig. 7. After each reaction, the catalyst was conveniently separated with a magnet, washed thoroughly with ethanol, dried under vacuum and reused for the subsequent cycles. It is confirmed that the styrene conversion and selectivity more or less remain the same even after using for 5 consecutive cycles, suggesting outstanding stability and recyclability of the ZC-700 catalyst. Besides, leaching experiment was performed to verify the heterogeneity of the catalytic process. Initially, styrene (2 mmol) and the ZC-700 (50 mg) were added into DMF solution (8 mL) refluxed at 100 °C and air was introduced with a stable flowing rate of 80 mL min⁻¹. After 2 h the ZC-700 catalyst was removed by magnet separation under hot solution, and the reaction proceeded for another 4 h (Fig. 8), where no visible improvement in styrene conversion is observed. In addition, the result of ICP-AES analysis revealed the concentration of Co (II) ions in the supernatant corresponds to negligible catalyst leaching (0.32 ppm). These results indicate that ZC-700 catalyst is rather stable in the catalytic process

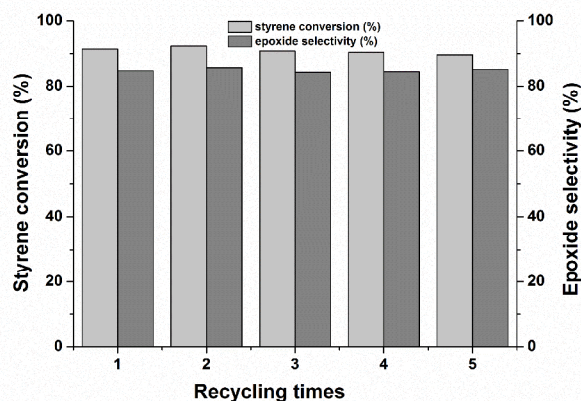


Fig. 7 Recycling experiments of ZC-700 catalyst for the epoxidation of styrene with air.

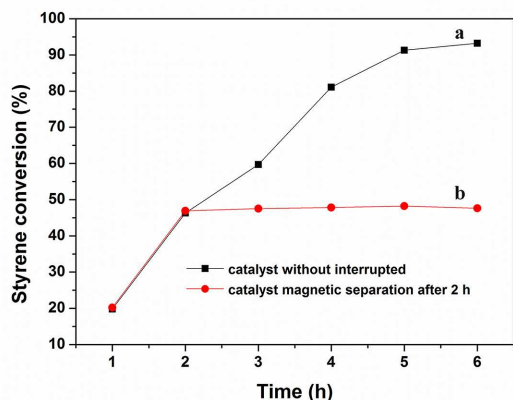


Fig. 8 (a) Kinetic profile of aerobic epoxidation of styrene and (b) leaching experiment of ZC-700 (continuing the reaction after the catalysts removing after 2 h).

Conclusions

Summary, in this contribution, we successfully established a simple and efficient strategy for the fabrication of well-structured nitrogen-cobalt catalysts with significantly and uniformly distributed catalytic center. Appropriate calcination temperature has been demonstrated to be principal factor for achieving nitrogen-cobalt macrocyclic catalysts with high selectivity and conversion. ZC-700 catalyst exhibits extraordinary good properties in styrene epoxidation under relatively mild conditions thanks to the effective active sites. Also, air as a final oxidant is suitable and offers practical benefits for this process. It highlights that the ferromagnetic characteristics of nitrogen-cobalt catalysts can be used for magnetic separation of catalyst, and reused 5 times with little or no loss in catalytic activity and epoxide selectivity. These results undoubtedly prove that MOFs-templated synthetic strategy empowers it to be facily extended to the preparation of other porous catalysts with well-defined structures and high-performance, and this process is effortlessly scalable for the catalyst industry.

Acknowledgements

We are grateful to the financial supports from National Basic Research Program of China (973 Program, grant no.2012CB821700), and NSFC project (grant no. 21120102034, 20831002).

Notes and references

- ^a Address Key State Key Laboratory of Inorganic Synthesis and Preparative Chemistry, College of Chemistry, Jilin University, Changchun 130012, P. R. China. Tel: +86 43185168331; E-mail: zhugs@jlu.edu.cn (G.S. Zhu).
- ^b Address College of Chemistry, Jilin University, Changchun, 130023, P.R. China.

- Q.-H. Xia, H.-Q. Ge, C.-P. Ye, Z.-M. Liu and K.-X. Su, *Chem. Rev.*, 2005, **105**, 1603-1662.
- K. C. Gupta and A. K. Sutar, *Coord. Chem. Rev.*, 2008, **252**, 1420-1450.
- E. Rose, B. Andrioletti, S. Zrig and M. Quelquejeu-Etheve, *Chem. Soc. Rev.*, 2005, **34**, 573-583.
- R. A. Sheldon, *Springer*, 1993, **164**, 21-43.
- I. V. Khavrutskii, D. G. Musaev and K. Morokuma, *Proc. Natl. Acad. Sci.*, 2004, **101**, 5743-5748.
- S. Bhor, M. K. Tse, M. Klawonn, C. Döbler, W. Mägerlein and M. Beller, *Adv. Synth. Catal.*, 2004, **346**, 263-267.
- J. Sun, Q. Kan, Z. Li, G. Yu, H. Liu, X. Yang, Q. Huo and J. Guan, *RSC Adv.*, 2014, **4**, 2310-2317.

ARTICLE

8. L. Ma, F. Su, X. Zhang, D. Song, Y. Guo and J. Hu, *Microporous Mesoporous Mater.*, 2014, **184**, 37-46.
9. Q. Tang, Q. Zhang, H. Wu, Y. Wang, *J. Catal.*, 2005, **230**, 384-397.
10. Q. Tang, Y. Wang, J. Liang, P. Wang, Q. Zhang, H. Wan, *Chem. Commun.*, 2004, 440-441.
11. J. Sebastian, K. M. Jinka, R. V. Jasra, *J. Catal.*, 2006, **244**, 208-218.
12. H. Cui, Y. Zhang, L. Zhao, Y. Zhu, *Catal. Commun.*, 2011, **12** 417-420
13. K. M. Jinka, S. M. Pai, B. L. Newalkar, N. V. Choudary, R. V. Jasra, *Catal. Commun.*, 2010, **11**, 638-642
14. G. Ferey, *Chem. Soc. Rev.*, 2008, **37**, 191-214.
15. S. Achmann, G. Hagen, J. Kita, I. M. Malkowsky, C. Kiener and R. Moos, *Sensors*, 2009, **9**, 1574-1589.
16. N. L. Rosi, J. Eckert, M. Eddaoudi, D. T. Vodak, J. Kim, M. O'Keeffe and O. M. Yaghi, *Science*, 2003, **300**, 1127-1129.
17. M. Latroche, S. Surble, C. Serre, C. Mellot-Draznieks, P. L. Llewellyn, J. H. Lee, J-S. Chang, S. H. Jung and G. Ferey, *Angew. Chem. Int. Ed.*, 2006, **45**, 8227-8231.
18. A. C. McKinlay, R. E. Morris, P. Horcajada, G. Ferey, R. Gref, P. Couvreur and C. Serre, *Angew. Chem. Int. Ed.*, 2010, **49**, 6260-6266.
19. J. Lee, O. K. Farha, J. Roberts, K. A. Scheidt, S. T. Nguyen and J. T. Hupp, *Chem. Soc. Rev.*, 2009, **38**, 1450-1459.
20. F. Llabresixamena, O. Casanova, R. Galiassotailleur, H. Garcia and A. Corma, *J. Catal.*, 2008, **255**, 220-227.
21. P. Horcajada, S. Surble, C. Serre, D- Y. Hong, Y-K. Seo, J- S. Chang, J- M. Greneche, I. Margiolaki and G. Ferey, *Chem. Commun.*, 2007, 2820-2822.
22. C-D. Wu, A. Hu, L. Zhang and W. Lin, *J. Am. Chem. Soc.*, 2005, **127**, 8940-8941.
23. A. Dhakshinamoorthy, M. Alvaro and H. Garcia, *Catal. Sci. Technol.*, 2011, **1**, 856-867.
24. A. Dhakshinamoorthy, M. Opanasenko, J. Čejka and H. Garcia, *Catal. Sci. Technol.*, 2013, **3**, 2509-2540.
25. J. Zhang, A. V. Biradar, S. Pramanik, T. J. Emge, T. Asefa and J. Li, *Chem Commun*, 2012, **48**, 6541-6543
26. M. A. Gotthardt, A. Beilmann, R. Schoch, J. Engelke and W. Kleist, *RSC Adv.*, 2013, **3**, 10676-10679.
27. C. M. Granadeiro, A. D. S. Barbosa, P. Silva, F. A. A. Paz, V. K. Saini, J. Pires, B. de Castro, S. S. Balula and L. Cunha-Silva, *Appl. Catal., A*, 2013, **453**, 316-326.
28. Z. Sun, G. Li, H.-o. Liu and L. Liu, *Appl. Catal., A*, 2013, **466**, 98-104.
29. M. J. Beier, W. Kleist, M. T. Wharmby, R. Kissner, B. Kimmerle, P. A. Wright, J. Grunwaldt, A. Bäker, *Chem. Eur. J.*, 2012, **18**, 887-898
30. M. Tonigold, Y. Lu, B. Bredenkötter, B. Rieger, S. Bahnmüller, J. Hitzbleck, G. Langstein, D. Vollkmer, *Angew. Chem. Int. Ed.*, 2009, **48**, 7546-7550
31. M. Tonigold, Y. Lu, A. Mavrandonakis, A. Puls, R. Staudt, J. Möllmer, J. Sauer, D. Volkmer, *Chem. Eur. J.*, 2011, **17**, 8671-8695
32. N. L. Torad, R. R. Salunkhe, Y. Li, H. Hamoudi, M. Imura, Y. Sakka, C. Hu, Y. Yamauchi, *Chem. Eur. J.*, 2014, **20**, 7895-7900
33. N. L. Torad, M. Hu, S. Ishihara, H. Sukegawa, A. A. Belik, M. Imura, K. Ariga, Y. Sakka, Y. Yamauchi, *small*, 2014, **10**, 2096-2107
34. G. F. Wang, N. Ramesh, A. Hsu, D. Chu and R. R. Chen, *Mol. Simul.*, 2008, **34**, 1051-1056.
35. R. Banerjee, A. Phan, B. Wang, C. Knobler, H. Furukawa, M. O'Keeffe and O. M. Yaghi, *Science*, 2008, **319**, 939-943.
36. H. Cui, Y. Zhang, Z. Qiu, L. Zhao, Y. Zhu, *Appl. Catal., B*, 2010, **101**, 45-53
37. S. Ma, G. A. Goenaga, A. V. Call and D-J. Liu, *Chem. Eur. J.*, 2011, **17**, 2063-2067.
38. W. Xia, J. Zhu, W. Guo, L. An, D. Xia, R. Zou, *J. Mater. Chem. A*, 2014, **2**, 11606-11613.
39. X. Wang, J. Zhou, H. Fu, W. Li, X. Fan, G. Xin, J. Zheng, X. Li, *J. Mater. Chem. A*, 2014, 10qw.1039/c0xx00000x
40. F. Su, C. K. Poh, J. S. Chen, G. Xu, D. Wang, Q. Li, J. Lin and X. W. Lou, *Energy Environ. Sci.*, 2011, **4**, 717-724.
41. Q. Liu and J. Zhang, *Langmuir*, 2013, **29**, 3821-3828.
42. A. Morozan, P. Jegou, B. Jusselme and S. Palacin, *Phys. Chem. Chem. Phys.*, 2011, **13**, 21600-21607.
43. M. Yuasa, A. Yamaguchi, H. Itsuki, K. Tanaka, M. Yamamoto and K. Oyaizu, *Chem. Mater.*, 2005, **17**, 4278-4281.
44. R. Nie, J. Shi, W. Du, W. Ning, Z. Hou and F-S. Xiao, *J. Mater. Chem. A*, 2013, **1**, 9037-9045.
45. J-H. Yang, G. Sun, Y. Gao, H. Zhao, P. Tang, J. Tan, A-H. Lu and D. Ma, *Energy Environ. Sci.*, 2013, **6**, 793-798.
46. S. Li, L. Zhang, J. Kim, M. Pan, Z. Shi and J. Zhang, *Electrochim. Acta*, 2010, **55**, 7346-7353.
47. J. Sun, G. Yu, L.Liu, Z. Li, Q. Kan, Q. Huo, J. Guan, *Catal. Sci. Technol.*, 2014, **4** 1246-1252.
48. X-H. Lu, Q-H. Xia, D. Zhou, S-Y. Fang, A-L. Chen, Y-L. Dong, *Catal. Commun.*, 2009, **11**, 106-109.
49. D. Zhou, B. Tang, X-H. Lu, X-L. Wei, K. Li, Q-H. Xia, *Catal. Commun.*, 2014, **45**, 124-128.